Author Manuscript

Author Manuscript

Author Manuscript

Author Manuscript

HHS Public Access

Author manuscript

Acad Radiol. Author manuscript; available in PMC 2016 July 01.

Published in final edited form as:

Acad Radiol. 2015 July ; 22(7): 853–859. doi:10.1016/j.acra.2015.02.012.

Prone Versus Supine Breast FDG-PET/CT for Assessing Locoregional Disease Distribution in Locally Advanced Breast Cancer

Richard G. Abramson, MD,
Department of Radiology and Radiological Sciences, Vanderbilt University, 1161 21st Ave. S, CCC-1121 MCN, Nashville, TN 37232-2675, (615) 322-6759, Fax (615) 322-3764, richard.abramson@vanderbilt.edu

Katrina F. Lambert, MD,
Department of Radiology and Radiological Sciences, Vanderbilt University, 1161 21st Ave. S, CCC-1121 MCN, Nashville, TN 37232-2675, katrina.f.lambert@vanderbilt.edu

Laurie B. Jones-Jackson, MD,
Department of Radiology and Radiological Sciences, Vanderbilt University, 1161 21st Ave. S, CCC-1121 MCN, Nashville, TN 37232-2675, laurie.b.jones-jackson@vanderbilt.edu

Lori R. Arlinghaus, PhD,
Institute of Imaging Science, Vanderbilt University, 1161 21st Ave South, AA-1105 MCN, Nashville, TN 37232-2310, lori.arlinghaus@vanderbilt.edu

Jason Williams, PhD,
Institute of Imaging Science, Vanderbilt University, 1161 21st Ave South, AA-1105 MCN, Nashville, TN 37232-2310, jason.williams@vanderbilt.edu

Vandana G. Abramson, MD,
Vanderbilt-Ingram Cancer Center, 2220 Pierce Ave, 777 PRB, Nashville, TN 37232-6848, vandana.abramson@vanderbilt.edu

A. Bapsi Chakravarthy, MD, and
Vanderbilt University Medical Center, Department of Radiation Oncology, 1301 22nd Ave South, B1003, Nashville, TN 37323-5671, bapsi.chak@vanderbilt.edu

Thomas E. Yankeelov, PhD
Vanderbilt University Institute of Imaging Science, 1161 21st Ave South, AA-1105 MCN, Nashville, TN 37232-2310, tom.yankeelov@vanderbilt.edu

Abstract

© 2015 Published by AUR.

Correspondence to: Richard G. Abramson.

Publisher's Disclaimer: This is a PDF file of an unedited manuscript that has been accepted for publication. As a service to our customers we are providing this early version of the manuscript. The manuscript will undergo copyediting, typesetting, and review of the resulting proof before it is published in its final citable form. Please note that during the production process errors may be discovered which could affect the content, and all legal disclaimers that apply to the journal pertain.

Author Manuscript Author Manuscript Author Manuscript Author Manuscript

Rationale and Objectives—Prone F-18 fluorodeoxyglucose (FDG)-PET/CT may have advantages for breast imaging due to improved separation of deep anatomical structures. There are limited data on whether prone and supine FDG-PET/CT provide similar information regarding breast and axillary disease in the setting of locally advanced breast cancer (LABC). The purpose of this study was to compare the information on locoregional disease distribution provided by prone versus supine FDG-PET in newly diagnosed LABC.

Materials and Methods—In an IRB-approved prospective trial, 24 patients with newly diagnosed LABC underwent both supine and prone FDG-PET/CT at the same scanning session. Three readers performed an independent review of all scans and categorized the locoregional disease distribution as breast only (BO)-unifocal, BO-multifocal, BO-multicentric, or breast +axillary involvement. For breast+axillary disease, the readers also assessed the number of involved axillary lymph nodes. Inter-observer discrepancies were resolved at a consensus reading session.

Results—Two scanning sessions were excluded because the prone scan had omitted part of the axilla from the field of view. In the remaining 22 patients, the consensus categorization of anatomical disease distribution was concordant between prone and supine scanning in 21 patients (linear kappa 0.91 [0.79 – 1]). In the 16 patients with breast+axillary disease, equal numbers of involved lymph nodes were identified on prone and supine scanning in 12 patients, while in the remaining four patients, prone scanning resulted in a higher number of visualized lymph nodes.

Conclusions—Prone and supine FDG-PET/CT provided statistically identical information on locoregional disease distribution in LABC. However, prone scanning may perform better than supine for assessing the number of involved lymph nodes. Prone FDG-PET/CT may be useful in future clinical and research efforts, including hybrid PET-MRI applications.

Keywords

Neoadjuvant chemotherapy; radiation planning; risk stratification; nodal disease burden

INTRODUCTION

F-18 fluorodeoxyglucose positron emission tomography (FDG-PET) is useful for the initial staging of locally advanced breast cancer (LABC) as well as for restaging breast cancer in the setting of recurrence (1–3). FDG-PET is typically performed with the patient in the supine position, but some initial studies have suggested that prone scanning may be more effective in breast cancer due to better separation of deep breast tissue, axillary, and chest wall structures (4, 5). The recent introduction of hybrid PET-magnetic resonance imaging (MRI) scanners provides additional motivation for studying prone FDG-PET of the breast; as breast MRI is currently performed with the patient in the prone position, prone FDG-PET may achieve better anatomical correlation with prone breast MRI in hybrid imaging applications (6–8).

At present, there is limited data on whether prone FDG-PET provides the same information as supine FDG-PET on locoregional disease distribution in breast cancer. Although FDG-PET does not currently play a major role in the clinical assessment of tumor multifocality or axillary nodal staging, these are areas in which FDG-PET performance may improve and

Author Manuscript Author Manuscript Author Manuscript Author Manuscript

new FDG-PET indications may emerge, especially with the evolution of higher spatial resolution positron emission mammography (PEM) and hybrid PET-MRI systems (1, 8). We therefore undertook this study to compare the information offered by prone versus supine FDG-PET in the context of newly diagnosed LABC. We investigated differences between prone and supine scanning in (a) qualitative categorization of the anatomical distribution of disease and (b) assessment of the number of involved axillary lymph nodes.

MATERIALS AND METHODS

Patients

This IRB-approved, prospective study was conducted as part of a larger investigation of PET/CT as an early predictor of response in breast cancer patients undergoing neoadjuvant chemotherapy (NAC) (9). Inclusion criteria included age ≥ 18 years, biopsy-proven breast cancer, and locally advanced disease considered by the treating oncologist to merit consideration of NAC. Between November 2010 and July 2012, 24 patients with newly diagnosed LABC were enrolled on study. Written informed consent was obtained from each patient prior to enrollment.

FDG-PET Imaging

Initial staging FDG-PET/CT was performed between the time of histologic diagnosis and the initiation of NAC. At this scanning session, all patients underwent both prone and supine FDG-PET/CT on a GE Discovery STE scanner (GE Healthcare, Waukesha, WI, USA), with prone scanning performed prior to supine. FDG at a dose of 0.56 MBq/kg (0.15 mCi/kg) was administered intravenously via an antecubital vein contralateral to the affected breast. Patients then rested for approximately 60 minutes. With the patient in the prone position, scanning of the chest was performed. The patient was then immediately repositioned, and scanning of the whole body was performed with the patient in the supine position. Acquisition times and time delays between prone and supine scanning were recorded for each patient. Emission data were collected in 3-D mode for two minutes per bed position.

During prone scanning, the patients' breasts were positioned within a custom built support device (Fig. 1). This device allowed the breasts to hang pendant during the scanning procedure and was designed to facilitate registration with prone breast MRI (9). The device is an exact geometric replica of a 4-channel receiver double-breast radiofrequency coil (In Vivo, Inc., Gainesville, FL, USA) used on the Philips 3T Achieva MR scanner (Philips Healthcare, Best, The Netherlands). It was constructed from lightweight, rigid polystyrene foam insulation (McMaster, Atlanta, GA, USA) that was machined to match the dimensions of the MRI breast coil and then surrounded with a set of MRI coil padding. The fully constructed support device was assessed for CT attenuation by a certified PET/CT technologist.

In conjunction with the PET acquisition, a low-mAs CT scan was acquired for attenuation correction of the emission data. Transmission CT parameters were: tube voltage 120 kVp, tube current scaled according to patient weight (80 mAs for 70-kg patient), and pitch 1.675:1.

Author Manuscript Author Manuscript Author Manuscript Author Manuscript

Data Extraction

Three readers (one board-certified nuclear medicine physician, one board-certified diagnostic radiologist, and one diagnostic radiology resident) performed independent reviews of all scans and qualitatively categorized the anatomical distribution of disease using the following designations: breast only (BO)-unifocal, BO-multifocal, BO-multicentric, or breast+axillary involvement. Multifocal disease was defined as disease limited to one breast quadrant. Multicentric disease was defined as disease in more than one breast quadrant.

For breast+axillary disease, the readers also assessed the number of involved lymph nodes, defined as the number of lymph nodes demonstrating subjectively abnormal metabolic activity relative to background, i.e., without reference to a quantitative standardized uptake value (SUV) threshold. Information from low-dose CT was incorporated for anatomical localization and also for decision-making in cases where lymph node involvement was equivocal. (Lymph nodes with borderline abnormal metabolic activity were considered more likely to be metastatic if they demonstrated rounded morphology or measured ≥ 10 mm in short axis.) Inter-observer discrepancies were resolved at a consensus reading session with all three readers in attendance.

Statistical Analysis

Statistical analyses were performed using publicly available software (www.vassarstats.net). The kappa test with linear weighting was used to compare the qualitative categorization of anatomical disease distribution between prone and supine scanning. The Wilcoxon signed-rank test was used to compare assessments of the number of involved lymph nodes on prone and supine scans. $P < 0.05$ was considered statistically significant.

RESULTS

Patient and Tumor Characteristics

Patient demographic information and tumor characteristics are summarized in Table 1. Median patient age was 47 years (range 32 to 67). Size of the primary tumor ranged from 1.3 cm to 10 cm. All tumors were high or intermediate-grade invasive mammary carcinomas of no special histologic type, with the exception of one invasive lobular carcinoma. The sample contained a heterogeneous group of tumors by receptor overexpression, as detailed in Table 1.

Acquisition Times

Scan acquisition times are summarized in Table 2. Prone acquisitions were initiated at a median 62.15 minutes following injection of ^{18}F-FDG (range 54.50 – 78.2 minutes). Supine injections were initiated at a median 73.09 minutes following injection (range 65.82 – 92.35 minutes). The median delay between prone and supine scans was 11.23 minutes (range 9.68 – 21.18 minutes).

Author Manuscript Author Manuscript Author Manuscript Author Manuscript

Scan Quality

22 out of 24 scanning sessions were considered acceptable for inclusion in subsequent data analyses. The remaining two scanning sessions were excluded because the prone scan had omitted part of the axilla from the field of view resulting in some information loss (Fig. 2). This exclusion is addressed in the Discussion below.

Categorization of Anatomical Disease Distribution

Table 3 summarizes the observers' consensus categorizations of anatomical disease distribution. Categorization was concordant between prone and supine scanning in 21 of 22 patients (linear kappa 0.91, 95% confidence interval [0.79 – 1]). Patient C was discordantly categorized as BO-multifocal on prone scanning and BO-unifocal on supine; this patient's tumor was a low-grade invasive lobular carcinoma with very low metabolic activity, and the prone scan may have had some motion artifact (Fig. 3).

Assessment of Number of Involved Lymph Nodes

Table 4 summarizes the observers' consensus assessments of the number of involved lymph nodes in the 16 patients with breast+axillary disease. In 12 out of the 16 patients, equal numbers of involved lymph nodes were identified on prone and supine scanning ($p > 0.5$). In the remaining four patients, prone scanning resulted in a higher number of visualized lymph nodes, with prone scanning thought to be superior on the basis of improved separation of deep anatomical structures (Fig. 4).

DISCUSSION

FDG-PET for breast cancer staging is typically performed in the supine position. Some studies have suggested, however, that emission breast imaging acquired in the prone position may be more effective due to better separation of deep anatomical structures. Khalkali et al. suggested that prone is preferable to supine imaging for diagnosing breast cancer with ^{99m}Tc-sestamibi scintigraphy (5). Yutani et al. compared prone to supine FDG-PET imaging for diagnosing breast cancer and found that although there was equivalent yield in both positions for detecting histologically confirmed breast cancers, prone acquisitions were associated with higher standardized uptake values (SUV) and tumor-to-normal tissue counts (4).

The emergence of hybrid PET-MRI systems (8) has further motivated the investigation of prone FDG-PET imaging in breast cancer. Prone FDG-PET may achieve better anatomical correlation with MRI data acquired in the same prone position, may facilitate better understanding of how PET and MRI metrics correlate both temporally and spatially, and may promote increased diagnostic performance through combined PET-MRI acquisition (8). Moy et al. used a prone breast positioning device and reported in a small series that fused images from prone FDG-PET and prone MRI increased their confidence in characterizing a lesion as benign or malignant, while fused images using supine FDG-PET were not interpretable due to architectural distortion of the breasts (6). The same group reported separately that fusion of images with prone FDG-PET increased the specificity of MRI but decreased its sensitivity (7).

Author Manuscript Author Manuscript Author Manuscript Author Manuscript

To our knowledge, this is the first attempt to compare prone and supine FDG-PET for providing information on locoregional disease distribution in the setting of recently diagnosed LABC. This study is clinically relevant when considering the possible future roles that FDG-PET may play in breast cancer treatment planning and risk stratification. At the present time, the role of FDG-PET imaging for regional breast cancer staging is quite limited: the spatial resolution of traditional FDG-PET is considered inadequate for assessing primary tumor size (1), and FDG-PET is not currently considered a viable substitute for sentinel lymph node sampling to evaluate for axillary nodal involvement (10). However, recent studies have suggested that FDG-PET may be of value in treatment planning by revealing otherwise undiagnosed multifocal disease (11), and one recent series showed that FDG-PET assessed lesion multifocality better than MRI (12). With increasing spatial resolution, FDG-PET may be incorporated in the future into risk stratification models that include, among other variables, estimates of the number of pathologic lymph nodes at the time of diagnosis (13). Prone FDG-PET may improve diagnostic performance for evaluating both primary tumor status and axillary lymph node involvement by separating anatomical structures and by facilitating coregistration with prone MRI data in new hybrid PET-MRI applications.

In our patient sample, we found that prone and supine FDG-PET achieved very high concordance in categorizing anatomical disease distribution into BO-unifocal, BO-multifocal, BO-multicentric, or breast+axillary involvement. A discordant categorization occurred in only one patient with a low-grade invasive lobular carcinoma. This tumor had very low metabolic activity and was difficult to discriminate from background parenchyma even in retrospect, thus highlighting the known limitations of FDG-PET for imaging of invasive lobular breast carcinomas (11).

In the quantitative assessment of involved axillary lymph nodes, we found less concordance between prone and supine scanning. Prone imaging revealed a higher number of visualized lymph nodes in four out of 16 patients with breast+axillary disease, presumably due to improved separation of deep structures. This is a potentially important result because accurate quantification of involved axillary lymph nodes feeds directly into decision-making regarding post-mastectomy adjuvant radiation therapy. Recommendations regarding post-mastectomy radiation are currently based on large randomized trials involving patients who did not receive NAC; in this setting, patients with four or more positive nodes at the time of surgery are thought to have a sufficiently high risk of local recurrence to warrant adjuvant radiation (14, 15). For patients who receive NAC prior to mastectomy, however, the paradigm is more complicated and remains an area of active investigation. Radiation recommendations for these patients are currently based on pretreatment clinical staging, since by the time of surgery patients may have already demonstrated significant NAC-related changes in pathological extent of disease (16). FDG-PET thus has significant opportunity for improvement over current clinical methods of quantifying nodal disease burden prior to initiation of NAC. As a substitute for (or adjunct to) clinical staging, pre-treatment FDG-PET may be used in future risk stratification models and may eventually be used to inform radiation treatment decisions in the adjuvant setting. Our results suggest that prone FDG-PET may perform better than supine in this context. The stage is thus set for further evaluation of prone FDG-PET both in isolation and combined with prone MRI for

Author Manuscript Author Manuscript Author Manuscript Author Manuscript

quantification of nodal disease at the time of initial staging. Further investigation would ideally lead to a formal comparative effectiveness analysis evaluating the effect of initial noninvasive FDG-PET staging on patient outcomes.

A final important result from our study was the need to exclude two scanning sessions from analysis due to omission of part of the axilla from the field of view on the prone scan. This observation underscores the need for close attention to the field of view during prone acquisitions to account for shifts of anatomical structures with different patient positions.

This preliminary study has several potential limitations. First, we were unable to compare prone and supine scanning against a pathological gold standard because all patients on this study proceeded to NAC immediately after the initial staging scans. Second, our sample was small and contained a heterogeneous group of breast cancer subtypes. Third, our scanning protocol (prone scanning followed by supine) raises the possibility that the order of acquisition may have biased our results. (We were unable to vary the scanning order due to the need to maintain a standardized imaging protocol for our larger, ongoing investigation of PET/CT as an early predictor of treatment response.) We suggest, however, that any bias from our scanning order would have favored the supine acquisition over the prone, given that breast malignancies have been shown to accumulate ^{18}F-FDG over time on dual-time-point FDG-PET imaging (17). We believe that in this study, the short amount of time between the two scans (median: 11 minutes) would have had a negligible effect on intralesional ^{18}F-FDG accumulation.

In conclusion, our study suggests that prone FDG-PET provides similar information to supine FDG-PET for the anatomical categorization of disease in the setting of newly diagnosed LABC, and that prone FDG-PET may be superior for quantification of involved axillary lymph nodes due to better separation of deep breast tissue, axillary, and chest wall structures. However, caution must be exercised with defining the field of view in prone scanning, given shifts of anatomical structures with changes in patient positioning. Finally, as has been previously reported, the accuracy of both supine and prone FDG-PET is limited in the setting of invasive lobular breast carcinomas given their low metabolic activity. Our results require confirmation in a larger trial given our small sample size and heterogeneous group of breast cancer subtypes, but lend justification to further investigation of prone FDG-PET imaging in the setting of newly diagnosed LABC.

ACKNOWLEDGEMENTS

We offer our most sincere gratitude to the women who participate in our studies. We also thank the National Institutes of Health for funding through NCI 1R01CA129961, NCI U01 CA142565, NCI 1U01CA174706, NCI P50 CA098131 and NCI P30 CA68485. We thank the Kleberg Foundation for its generous support of the molecularly imaging program at our institution. We gratefully acknowledge Pei-Fang Su, Ph.D., for assisting us in our choice of statistical methods, and Dominique Delbeke, M.D., Ph.D., for comments on an earlier version of this manuscript. RGA was funded in part by the AUR-GE Radiology Research Academic Fellowship.

REFERENCES

1. Groheux D, Espie M, Giacchetti S, Hindie E. Performance of FDG PET/CT in the clinical management of breast cancer. Radiology. 2013; 266(2):388–405. [PubMed: 23220901]

Author Manuscript Author Manuscript Author Manuscript Author Manuscript

2. Hegarty C, Collins CD. PET/CT and breast cancer. Cancer Imaging. 2010; 10(Spec no A):S59–S62. [PubMed: 20880780]

3. Fletcher JW, Djulbegovic B, Soares HP, et al. Recommendations on the use of 18F-FDG PET in oncology. Journal of nuclear medicine : official publication, Society of Nuclear Medicine. 2008; 49(3):480–508.

4. Yutani K, Tatsumi M, Uehara T, Nishimura T. Effect of patients' being prone during FDG PET for the diagnosis of breast cancer. AJR Am J Roentgenol. 1999; 173(5):1337–1339. [PubMed: 10541114]

5. Khalkhali I, Mena I, Diggles L. Review of imaging techniques for the diagnosis of breast cancer: a new role of prone scintimammography using technetium-99m sestamibi. European journal of nuclear medicine. 1994; 21(4):357–362. [PubMed: 8005161]

6. Moy L, Noz ME, Maguire GQ Jr, et al. Prone mammoPET acquisition improves the ability to fuse MRI and PET breast scans. Clinical nuclear medicine. 2007; 32(3):194–198. [PubMed: 17314593]

7. Moy L, Ponzo F, Noz ME, et al. Improving specificity of breast MRI using prone PET and fused MRI and PET 3D volume datasets. Journal of nuclear medicine : official publication, Society of Nuclear Medicine. 2007; 48(4):528–537.

8. Yankeelov TE, Peterson TE, Abramson RG, et al. Simultaneous PET-MRI in oncology: a solution looking for a problem? Magnetic resonance imaging. 2012; 30(9):1342–1356. [PubMed: 22795930]

9. Li X, Abramson RG, Arlinghaus LR, et al. An algorithm for longitudinal registration of PET/CT images acquired during neoadjuvant chemotherapy in breast cancer: preliminary results. EJNMMI research. 2012; 2(1):62. [PubMed: 23157877]

10. Wahl RL, Siegel BA, Coleman RE, Gatsonis CG. Prospective multicenter study of axillary nodal staging by positron emission tomography in breast cancer: a report of the staging breast cancer with PET Study Group. Journal of clinical oncology : official journal of the American Society of Clinical Oncology. 2004; 22(2):277–285. [PubMed: 14722036]

11. Groves AM, Shastry M, Ben-Haim S, et al. Defining the role of PET-CT in staging early breast cancer. Oncologist. 2012; 17(5):613–619. [PubMed: 22539550]

12. Heusner TA, Kuemmel S, Umutlu L, et al. Breast cancer staging in a single session: whole-body PET/CT mammography. Journal of nuclear medicine : official publication, Society of Nuclear Medicine. 2008; 49(8):1215–1222.

13. Ravdin PM, Siminoff LA, Davis GJ, et al. Computer program to assist in making decisions about adjuvant therapy for women with early breast cancer. Journal of clinical oncology : official journal of the American Society of Clinical Oncology. 2001; 19(4):980–991. [PubMed: 11181660]

14. Recht A, Edge SB, Solin LJ, et al. Postmastectomy radiotherapy: clinical practice guidelines of the American Society of Clinical Oncology. Journal of clinical oncology : official journal of the American Society of Clinical Oncology. 2001; 19(5):1539–1569. [PubMed: 11230499]

15. Aebi S, Davidson T, Gruber G, Cardoso F. Primary breast cancer: ESMO Clinical Practice Guidelines for diagnosis, treatment and follow-up. Annals of oncology : official journal of the European Society for Medical Oncology / ESMO. 2011; 22(Suppl 6):vi12–vi24. [PubMed: 21908498]

16. Huang EH, Tucker SL, Strom EA, et al. Postmastectomy radiation improves local-regional control and survival for selected patients with locally advanced breast cancer treated with neoadjuvant chemotherapy and mastectomy. Journal of clinical oncology : official journal of the American Society of Clinical Oncology. 2004; 22(23):4691–4699. [PubMed: 15570071]

17. Imbriaco M, Caprio MG, Limite G, et al. Dual-time-point 18F-FDG PET/CT versus dynamic breast MRI of suspicious breast lesions. AJR Am J Roentgenol. 2008; 191(5):1323–1330. [PubMed: 18941064]

Author Manuscript Author Manuscript Author Manuscript Author Manuscript

Figure 1.
Custom-built breast support device for acquiring prone PET-CT images. It allows the breasts to lie pendant during the scanning procedure, thus replicating anatomical positioning during prone breast MRI.

Author Manuscript Author Manuscript Author Manuscript Author Manuscript

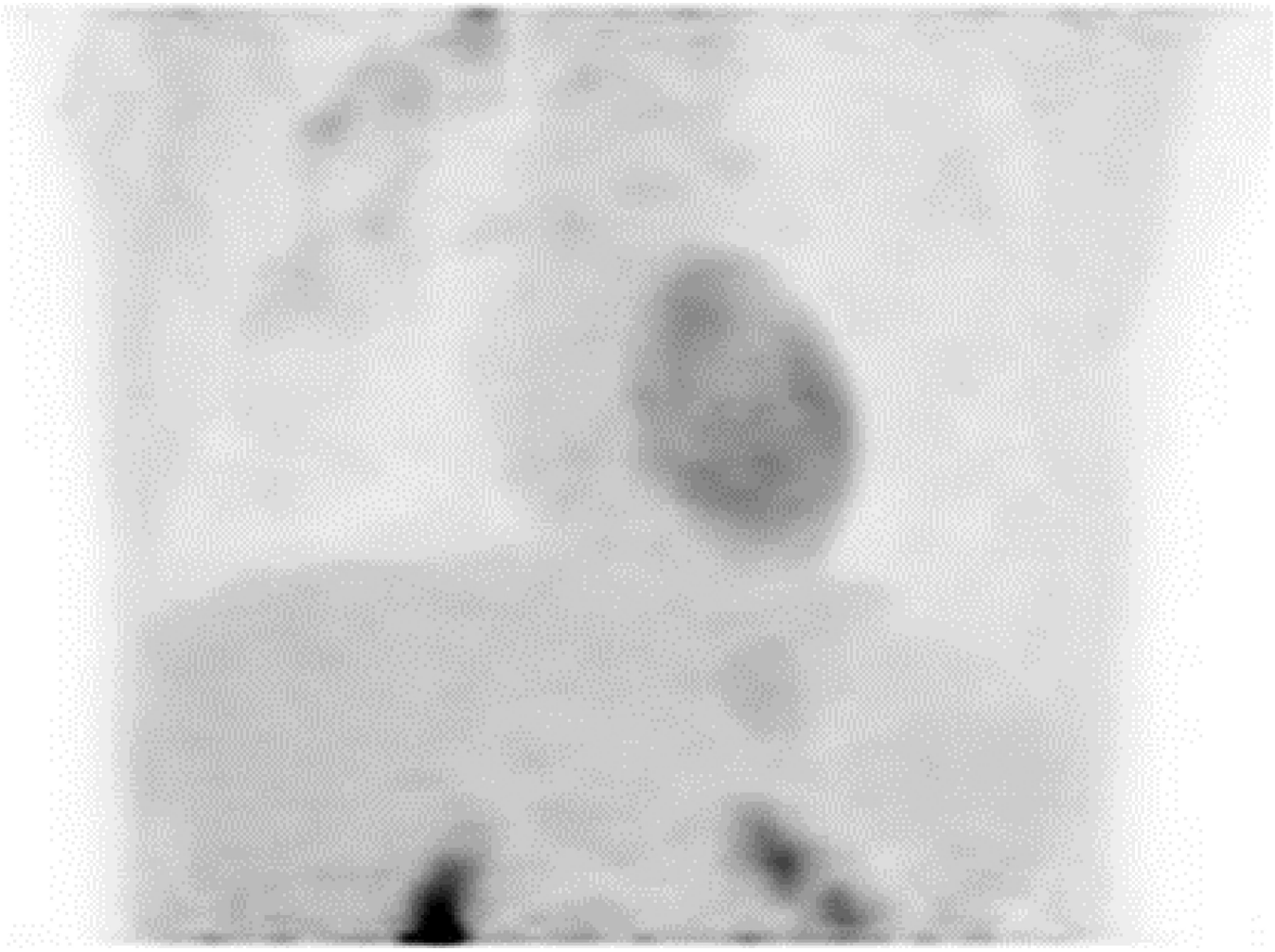

Author Manuscript Author Manuscript Author Manuscript Author Manuscript

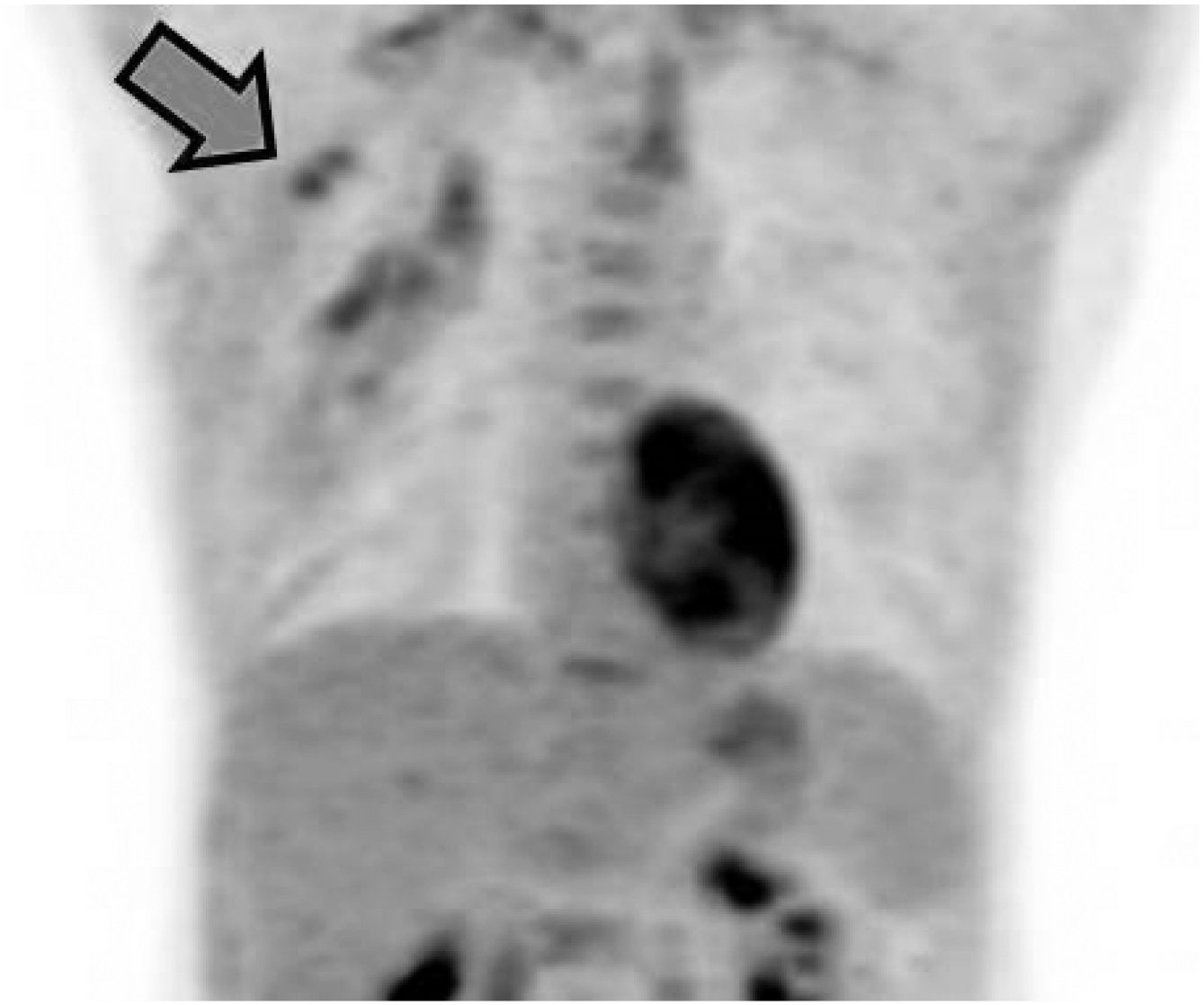

Figure 2.

A 48-year-old patient (Patient P) with a high-grade invasive mammary carcinoma of the right breast. Frontal three-dimensional maximum intensity projection (MIP) reconstructions from ^{18}F-FDG-PET imaging acquired in the (A) prone and (B) supine positions. Two right axillary lymph nodes seen on the supine scan (arrow) were excluded from the field of view on the prone scan.

Author Manuscript Author Manuscript Author Manuscript Author Manuscript

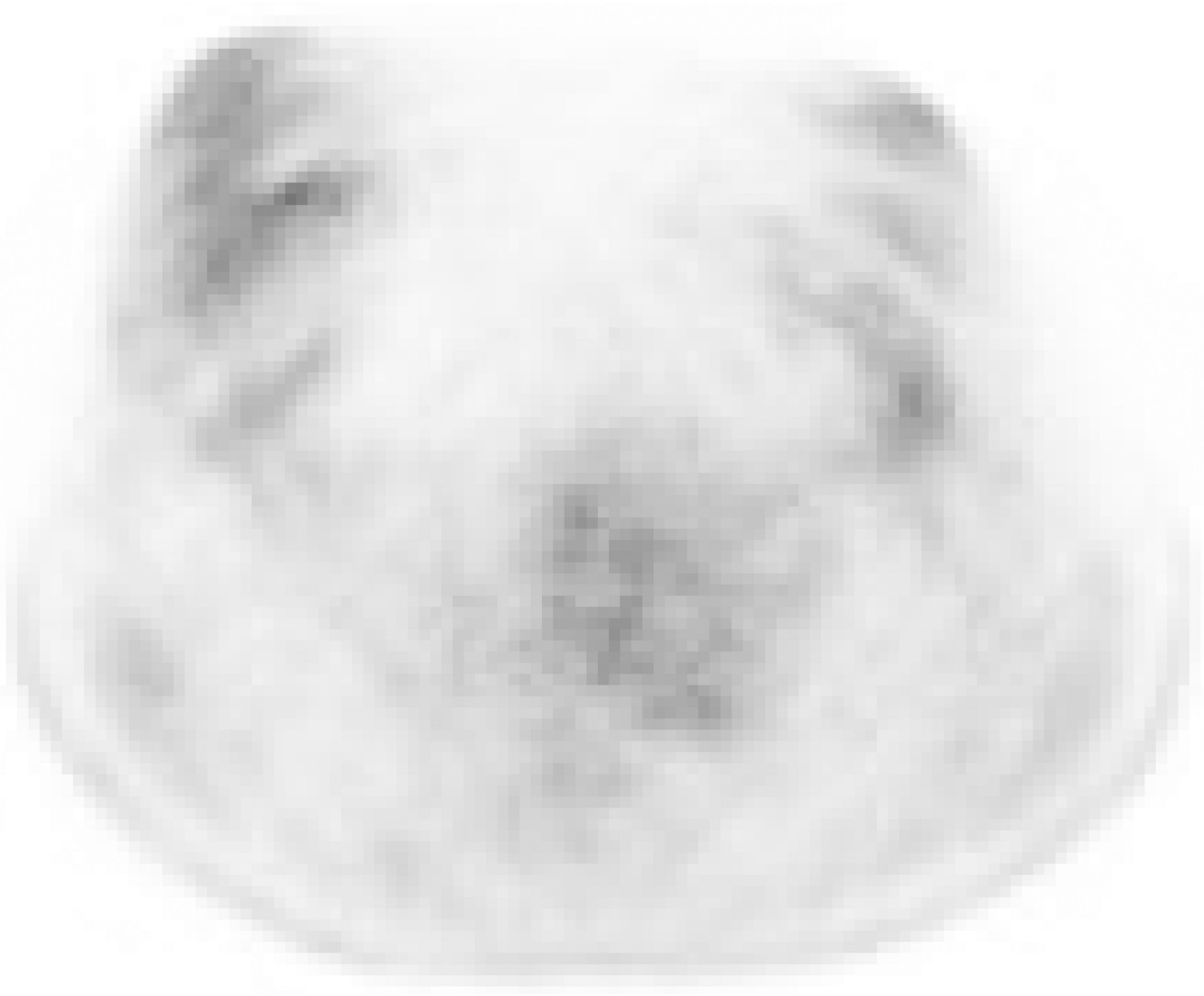

Author Manuscript Author Manuscript Author Manuscript Author Manuscript

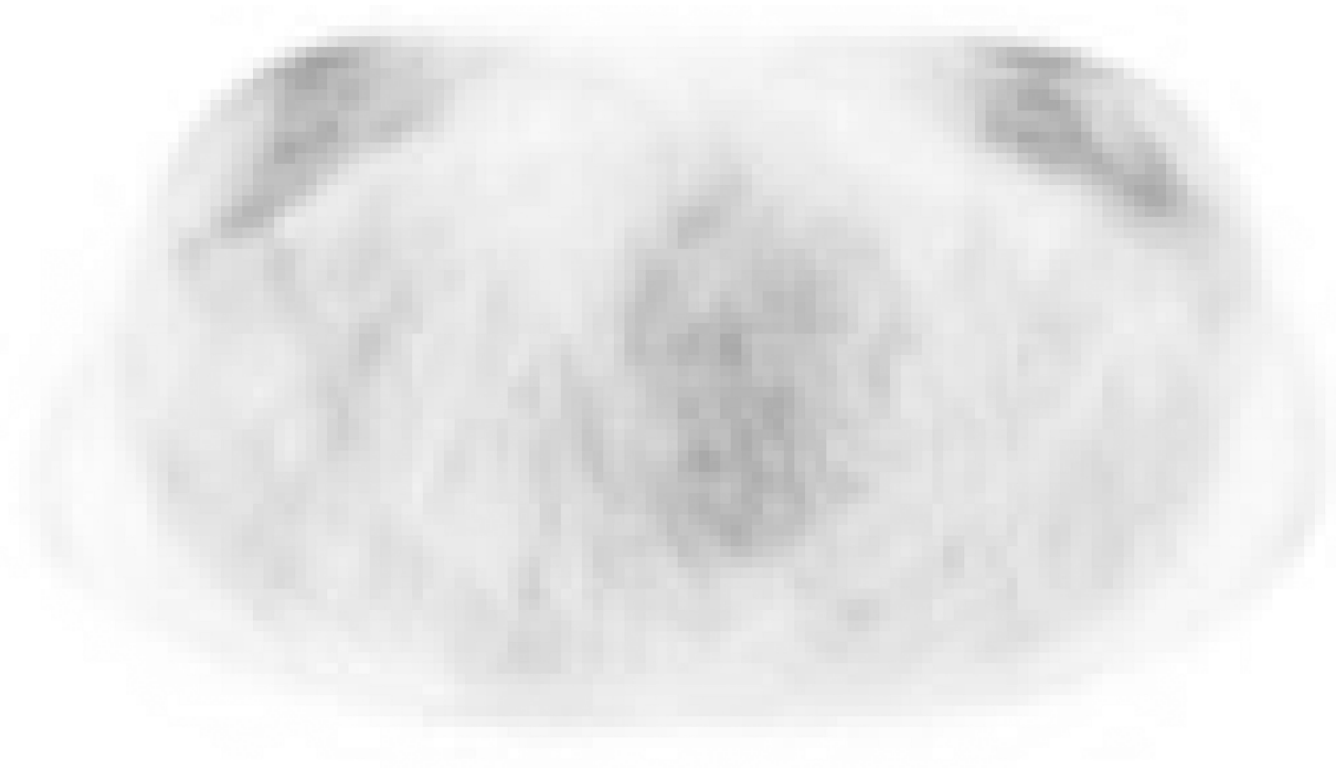

Figure 3.

A 39-year-old patient (Patient C) with a 10 cm low-grade invasive lobular carcinoma of the right breast. ^{18}F-FDG-PET imaging acquired in the (A) prone and (B) supine positions. This tumor exhibited very low metabolic activity and was discordantly categorized as having multifocal distribution on prone scanning but unifocal distribution on supine.

Author Manuscript Author Manuscript Author Manuscript Author Manuscript

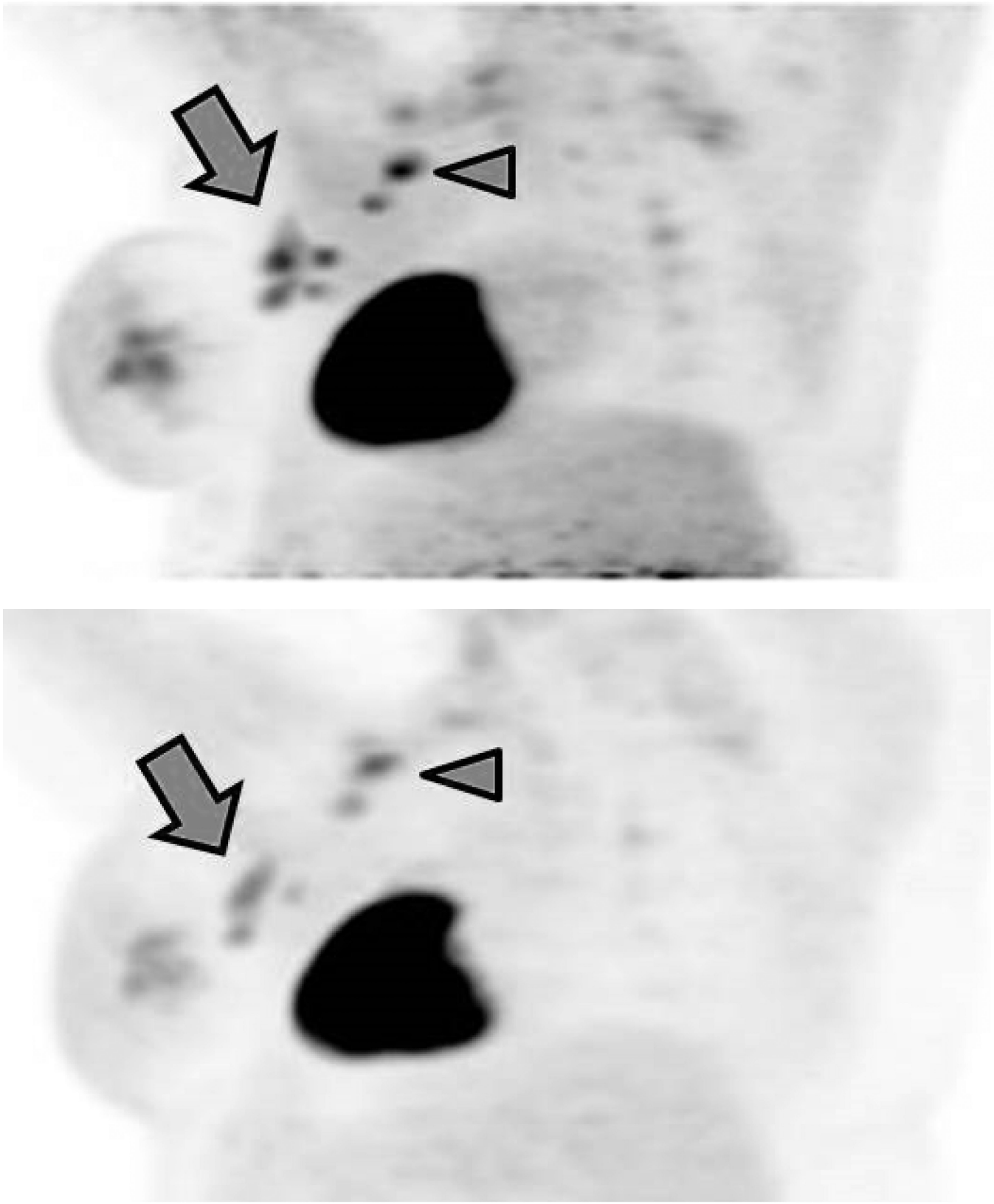

Figure 4.

Author Manuscript Author Manuscript Author Manuscript Author Manuscript

A 46-year-old patient (Patient B) with a high-grade invasive mammary carcinoma of the left breast. Oblique three-dimensional maximum intensity projection (MIP) reconstructions from ^{18}F-FDG-PET imaging acquired in the (A) prone and (B) supine positions. Four discrete hypermetabolic left axillary lymph nodes can be resolved on the prone scan but only three are visible on the supine scan (arrows). Two hypermetabolic supraclavicular lymph nodes are also noted (arrowheads).

Author Manuscript Author Manuscript Author Manuscript Author Manuscript

TABLE 1

Patient demographic information and tumor characteristics

Patient	Age	Diameter (technique)	Histologic type	Histologic grade	Proliferative rate	Receptor overexpression		
						ER	PR	HER2
A	48	4.2 cm (US)	IMC-NST	High	High	−	−	−
B	46	NDM	IMC-NST	High	Intermediate	+	+	+
C	39	10 cm (PE)	ILC	Low	Low	+	+	−
D	56	n/a	IMC-NST	High	Intermediate	+	−	+
E	54	9 cm (US)	IMC-NST	High	n/a	+	−	−
F	64	2 cm (US)	IMC-NST	High	n/a	−	−	−
G	32	2.9 cm (US)	IMC-NST	High	High	+	+	+
H	49	1.3 cm (US)	IMC-NST	High	Intermediate	−	−	+
I	67	2.4 cm (US)	IMC-NST	High	High	−	−	−
J	39	1.9 cm (MRI)	IMC-NST	High	Intermediate	−	−	−
K	33	4.3 cm (MRI)	IMC-NST	High	High	+	+	−
L	44	8 cm (PE)	IMC-NST	High	n/a	−	−	−
M	57	3 cm (US)	IMC-NST	High	High	−	−	−
N	43	1.8 cm (US)	IMC-NST	High	High	−	−	−
O	42	1.8 cm (US)	IMC-NST	High	High	−	−	−
P	48	NDM	IMC-NST	High	n/a	−	−	+
Q	45	3 cm (US)	IMC-NST	High	High	−	+	−
R	50	2 cm (MRI)	IMC-NST	Intermediate	Intermediate	−	−	−
S	55	3cm (US)	IMC-NST	Intermediate	Intermediate	+	+	−
T	43	2.9 cm (MRI)	IMC-NST	High	High	−	−	−
U	36	1.6 cm	IMC-NST	Intermediate	Low	+	+	−
V	65	4.6 cm	IMC-NST	Intermediate	Intermediate	−	−	+
W	42	3.6 cm	IMC-NST	Intermediate	Intermediate	+	+	−
X	56	n/a	IMC-NST	High	High	+	+	−

ER = estrogen receptor; HER2 = human epidermal growth factor receptor type 2; ILC = invasive lobular carcinoma; IMC-NST = invasive mammary carcinoma, no special type; MRI = magnetic resonance imaging; NDM = no discrete mass; n/a = not available; PE = physical examination; PR = progesterone receptor; US = ultrasound

Acad Radiol. Author manuscript; available in PMC 2016 July 01.

Author Manuscript

Author Manuscript

Author Manuscript

Author Manuscript

TABLE 2

Scan acquisition times

Patient	Start times (min after FDG injection)		Prone-supine delay (min)
	Prone	Supine	
A	64.48	77.25	12.77
B	61.05	72.78	11.73
C	64.8	76.28	11.48
D	70.38	85.73	15.35
E	58.05	79.23	21.18
F	61.15	73.17	12.02
G	71.02	81.23	10.21
H	60.23	71.75	11.52
I	61.88	71.62	9.74
J	64.27	75.32	11.05
K	62.48	73.00	10.52
L	64.5	74.95	10.45
M	62.48	73.00	10.52
N	54.5	65.98	11.48
O	55.32	65.82	10.50
P	59.98	69.83	9.85
Q	60.05	71.52	11.47
R	62.42	73.37	10.95
S	60.00	69.68	9.68
T	60.05	71.45	11.40
U	60.00	70.20	10.20
V	62.48	76.43	13.95
W	78.20	92.35	14.15
X	68.70	79.35	10.65

Author Manuscript

Author Manuscript

Author Manuscript

Author Manuscript

TABLE 3

Comparison of prone and supine scanning for categorization of anatomical disease distribution

Patient	Prone	Supine	Result	Comments
A	Breast+axilla	Breast+axilla	concordant	
B	Breast+axilla	Breast+axilla	concordant	
C	BO-multifocal	BO-unifocal	discordant	Low-grade invasive lobular carcinoma, very low metabolic activity
D	Breast+axilla	Breast+axilla	concordant	
E	Breast+axilla	Breast+axilla	concordant	
F	Breast+axilla	Breast+axilla	concordant	
G	Breast+axilla	Breast+axilla	concordant	
H	Breast+axilla	Breast+axilla	concordant	
I	--	--	--	Excluded due to part of axilla omitted from the field of view on prone scan
J	BO-unifocal	BO-unifocal	concordant	
K	Breast+axilla	Breast+axilla	concordant	
L	Breast+axilla	Breast+axilla	concordant	
M	Breast+axilla	Breast+axilla	concordant	
N	Breast+axilla	Breast+axilla	concordant	
O	BO-unifocal	BO-unifocal	concordant	
P	--	--	--	Excluded due to part of axilla omitted from the field of view on prone scan
Q	BO-unifocal	BO-unifocal	concordant	
R	BO-unifocal	BO-unifocal	concordant	
S	BO-unifocal (bilateral)	BO-unifocal (bilateral)	concordant	
T	Breast+axilla	Breast+axilla	concordant	
U	Breast+axilla	Breast+axilla	concordant	
V	Breast+axilla	Breast+axilla	concordant	
W	Breast+axilla	Breast+axilla	concordant	
X	Breast+axilla	Breast+axilla	concordant	

BO = breast only

Author Manuscript

Author Manuscript

Author Manuscript

Author Manuscript

TABLE 4

Comparison of prone and supine scanning for quantification of involved lymph nodes

Patient	Prone	Supine	Result	Comments
A	3	3	concordant	
B	6	5	discordant	Better anatomical separation of deep structures on prone scan
C	-	-		
D	1	1	concordant	
E	7	4	discordant	Better anatomical separation of deep structures on prone scan
F	4	3	discordant	Better anatomical separation of deep structures on prone scan
G	2	2	concordant	
H	1	1	concordant	
I	7	8	--	Excluded due to part of axilla omitted from the field of view on prone scan
J	-	-		
K	2	2	concordant	
L	2	2	concordant	
M	2	2	concordant	
N	1	1	concordant	
O	-	-		
P	0	3	--	Excluded due to part of axilla omitted from the field of view on prone scan
Q	-	-		
R	-	-		
S	-	-		
T	1	1	concordant	
U	9	5	discordant	Better anatomical separation of deep structures on prone scan
V	3	3	concordant	
W	4	4	concordant	
X	2	2	concordant	